

Numerical simulation of thermal runaway kinetic mechanisms and battery thermal model for safety assessment of different lithium-ion battery chemistries

S. Mehranfar*, A. Mahmoudzadeh Andwari*, J. Könnö *, A. Garcia Martinez **, C. Mico Reche**

* *Machine and Vehicle Design (MVD), Materials and Mechanical Engineering, Faculty of Technology, University of Oulu, FI-90014 Oulu, Finland (Sadegh Mehranfar Tel: +358 50 4321302; e-mail: Sadegh.Mehranfar@oulu.fi, Amin Mahmoudzadeh Andwari Amin.M.Andwari@oulu.fi)*

** *CMT–Clean Mobility and Thermo fluids. Universitat Politècnica de València. Camino de Vera s/n, 46022 Valencia, Spain*

Abstract: The importance of EVs and li-ion batteries are pinpointed in the automotive industry during the last decade by increased growth of electrified powertrain. Li-ion batteries offer significant improvements in terms of energy and power density; however, safety challenges continue to exist. Different thermal, mechanical, or electrical abuse conditions in li-ion batteries can trigger a series of exothermic chain reactions in the battery cells and finally result in thermal runaway (TR) and combustion of battery cells and EVs. Furthermore, different battery technologies exploit various cell chemistries, leading to the distinct thermal behavior of battery cells during normal and abuse conditions. This work aims at investigating the TR kinetic mechanisms to evaluate thermal behavior of the battery cells under thermal abuse conditions. Furthermore, this work investigates the different li-ion battery cathode, anode and electrolyte materials to assess the safety of battery systems in EV application. The results revealed that unlike batteries with LiCoO₂ cathodes with temperature threshold of 150 °C, Li_{1.1}(Ni_{1/3}Co_{1/3}Mn_{1/3})_{0.9}O₂ batteries do not undergo TR process at temperatures below 170 °C. Moreover, the temperature peak is more hazardous in LiCoO₂ batteries with LiPF₆/PC: DMC electrolyte compared to the same battery with standard electrolyte. In addition, batteries with Lithiated Li₄Ti₅O₁₂ anode showed safer TR process compared to all the previous battery types.

Keywords: Numerical simulation, Electric Vehicles, Li-ion batteries, Safety, Thermal runaway kinetic mechanisms

1. INTRODUCTION

The importance of EVs and li-ion batteries are pinpointed in the automotive section by the zero-tailpipe emission requirement of EU fleet and increased share of electrified powertrain in the market (IEA). Li-ion batteries offer significant improvements from the first generations of EVs in terms of energy density and power density, however, safety challenges in the way of li-ion EVs continue to exist (Wang et al., 2023). Extensive research has been done in thermal management of EV batteries by proposing hybrid cooling methods or even battery operating under cold climate to enhance the performance of battery system (Gharehghani et al., 2022, 2023). However, battery performance under abuse conditions remains a challenge for battery developers. Different thermal, mechanical, or electrical abuse conditions in li-ion batteries can trigger a series of exothermic chain reactions in the battery cells and finally result in thermal runaway (TR) and combustion of battery cell, battery system and the EV. Therefore, investigations of thermal behavior of battery cells under critical conditions are of utmost importance for EVs security and driver's safety. Moreover, different battery technologies exploit various cell chemistries (Cathode, anode, electrolyte and separator materials), leading to their distinct thermal behavior. Some researchers have

conducted investigations on the thermal behavior of Li-ion batteries under TR. A lumped model is proposed by Hatchard et al. (Hatchard et al., 2001) to model the oven test as a standard procedure of battery TR under thermal abuse conditions. Kim et al. extended the previous models to 3D models for oven tests of cylindrical cells and showed that smaller cylindrical cells can reject heat faster than larger cells and undergo a more moderate TR. Different studies have focused on the thermal stability of cathode materials. MacNiel et al. (MacNiel et al., 2002) studied the thermal stability of seven different cathode materials by differential scanning materials (DSC) and ranked them from safest to the least safe. Jiang et al. studied the three different cathode materials, LiCoO₂, Li(Ni_{0.1}Co_{0.8}Mn_{0.1})O₂ and LiFePO₄ using accelerated rate calorimetry (ARC) and showed that LiFePO₄ offers highest thermal stability. Peng et al. (Peng et al., 2016) numerically investigated thermal safety of batteries for five different cathode materials. Wang et al. (Wang et al., 2006) investigated the thermal stability of li-ion battery electrolytes and fitted the chemical reaction kinetics by Arrhenius law. They concluded that the stability of electrolyte plays a substantial role in li-ion safety. The effect of anode material was also investigated by Haung et al. (Haung et al., 2016). The thermal and combustion characteristics of TR over the battery module with Li₄Ti₅O₁₂ anode battery cells were investigated

through heating. Numerical investigation of thermal runaway behavior of lithium-ion batteries with different battery materials is also done by other researchers in the field (Kong et al., 2021). In spite of numerous research on the effect of battery material on the thermal stability of li-ion cells, a comprehensive study to investigate the effect of different cell components TR process of the battery cells is rarely done.

This work aims at the investigation of the most well-proven kinetic mechanism reactions of TR phenomena to evaluate thermal behavior of the battery cells with different materials under thermal abuse conditions. A thermal model with TR kinetic mechanism sub-model is adopted to replicate the behavior of the battery cells under thermal abuse conditions. Furthermore, to investigate the effect of different battery materials of the cell thermal behavior during TR, two different cathode, anode and electrolyte is selected from the literature and also their temperature evolution with heat rates are compared in the simulation of thermal abuse test. The results of this work will facilitate the integration of kinetic mechanisms into battery modelling under critical operation and will improve the safety design of li-ion batteries in EV application.

2. METHODOLOGY

This work employs a 2D thermal model integrated with the TR kinetic mechanism to evaluate the thermal stability of different li-ion battery cells under thermal abuse condition. The model was built in the commercial COMSOL Multiphysics software and by setting PDEs describing the undergoing physics of the problem. The simplified schematic of battery cell is presented in Fig.1 based on the 18,650-cell geometry and the model was developed by 2D definition.

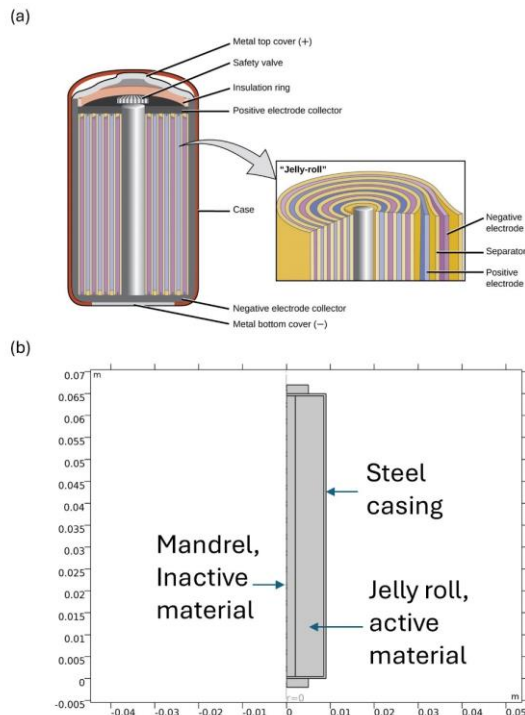


Fig. 1. A) Schematic of battery cell and inner structure B) Model Geometry of present work

The thermal model was adopted by defining the conservation of energy law and introducing the heat source term of TR reactions. Heat source term considers heat of reaction in TR event and by including a variety of different exothermic reactions in each component of battery. The objective of simulation is to replicate ARC test and trigger li-ion battery cells with thermal abuse and by setting oven temperature.

The interplay of heat transfer between cell and environment, heat of exothermic reactions and cell thermal balance determines the temperature dynamics of the cell. The temperature of the cell increases by the enthalpy of each reaction, which further increases the cell temperature and decreases the concentration of that component. The framework of numerical thermal model in the present study is illustrated in Fig. 2. Furthermore, li-ion cell properties in this simulation are listed in Table 1.

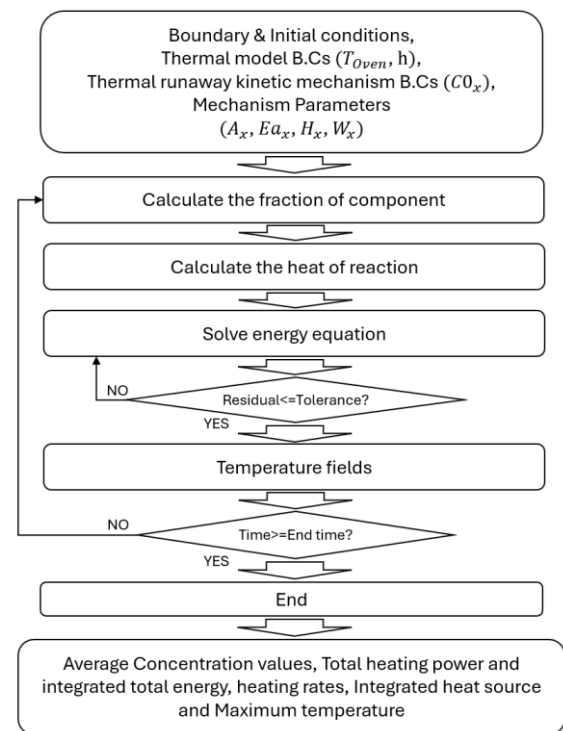


Fig. 2. Thermal modeling and TR framework

2.1 Thermal model

The thermal behavior inside the battery is modeled by the conduction heat transfer and conservation of energy as Eq.1 and 2. The generated heat Q_{gen} by decomposition of each component and dissipated heat Q_{diss} to the environment is then introduced into the energy equation.

$$\frac{dT_{Bat}}{dt} = \frac{Q_{gen} - Q_{diss}}{MC_p} \quad (1)$$

$$T_{Bat}(t) = T_{Bat,0} + \int \frac{dT_{Bat}}{dt} dt \quad (2)$$

The generated heat of each reaction is calculated by the TR model. Then, total generated heat is expressed as the

summation of multiple heat components following the following equation:

$$Q_{gen} = \sum Q_x \quad (3)$$

The interaction between battery and environment is determined by considering the convection and radiation heat as in Eq.4 and allows battery to reach to the environment temperature and calculate the released heat of reaction in that temperature. This iterative process is illustrated in Fig.2

$$Q_{diss} = Q_{conv} + Q_{rad} \\ = h \cdot A \cdot (T_{ARC} - T_{Bat}) \\ + \varepsilon \sigma (T_{ARC}^4 - T_{Bat}^4) \quad (4)$$

2.2 Thermal runaway model

The present model utilizes TR kinetic mechanisms introduced by Kim et al. (Kim et al., 2007). The model follows the basic kinetic mechanism of chemical reactions by the following Arrhenius form:

$$\kappa_x = \frac{dc_x}{dt} = A_x (c_x)^{n_1} (1 - c_x)^{n_2} e^{\frac{E_{a,x}}{R_0 T}} \quad (5)$$

Where κ_x is the reaction rate and c_x is the normalized concentration. Furthermore, A_x , E_a and g_x are the pre-exponential factor, activation energy and mechanism function respectively. The concentration of each species is then updated in the TR process as follows and by calculation of the reaction rate. Model parameters for Kim et al. mechanism is presented in Table 2 and.

$$c_x = 1 - \int \kappa_x dt \quad (6)$$

The heat of the reaction is then calculated by multiplication of reaction rate, heating value (H_x) and total mass of that component (m_x) as the following:

$$Q_x = m_x \cdot H_x \cdot \kappa_x \quad (7)$$

Finally, the generated heat of each reaction calculated by the model is superimposed to determine the total generated heat in the following equation:

$$Q_{gen} = \sum Q_x = Q_{SEI} + Q_a + Q_c + Q_e \quad (8)$$

Where Q_{SEI} is the heat from the SEI decomposition reaction, Q_a is the heat from the anode active material and electrolyte, Q_c is the heat from the cathode active material and electrolyte and Q_e is the heat from the electrolyte decomposition. The Model parameters of different battery materials are listed in Table 1.

The results of temperature evolution simulation are compared with the experimental data in Kim et al. (Kim et al., 2007) study. The comparison in Fig. 3 shows that temperatures in the simulation are in good agreement with the experimental data.

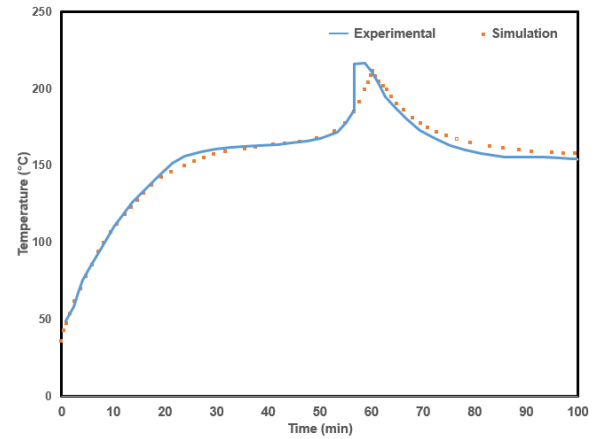


Fig. 3. Comparison of the simulated temperature and reference temperature for Kim et al. mechanism and Oven Temperature of 155 °C

In this study, a LiCoO_2 battery with standard LiPF_6 electrolyte and graphite anode is selected for oven test. Furthermore, a $\text{Li}_{1.1}(\text{Ni}_{1/3}\text{Co}_{1/3}\text{Mn}_{1/3})_{0.9}\text{O}_2$ cathode (Kong et al., 2021), LiPF_6/PC : DMC electrolyte (Wang et al., 2006) and lithiated $\text{Li}_4\text{Ti}_5\text{O}_{12}$ anode (Haug et al., 2016) is selected from the literature to assess the effect of different cathode, electrolyte and anode material on the thermal stability of the cell during thermal abuse conditions respectively. The Model parameters of different battery materials are listed in Table 1.

Table 1. Model parameters of different anode, cathode and electrolyte materials.

	Lithiated $\text{Li}_4\text{Ti}_5\text{O}_{12}$ anode (Haug et al., 2016)	$\text{Li}_{1.1}(\text{Ni}_{1/3}\text{Co}_{1/3}\text{Mn}_{1/3})_{0.9}\text{O}_2$ cathode (Kong et al., 2021)	LiPF_6/PC : DMC electrolyte (Wang et al., 2006)
H_x	2.568×10^5	7.9×10^5	3.209×10^5
A_x	5.21×10^{19}	2.25×10^{14}	7.53×10^{19}
E_x	1.88×10^5	1.54×10^5	1.882×10^5
W_x	1.274×10^3	1.293×10^3	0.96×10^3

Table 2. Model parameters and Li-ion cell properties for Kim et al. (Kim et al., 2007) mechanism.

Symbol	Description	Value
Cell format	18,650	-
Battery radius, m	r_{batt}	0.009
Battery height, m	h_{batt}	0.065
Thickness of battery can, m	d_{can}	$5E-4$
Mandrel radius, m	$r_{mandrel}$	0.002
Volumetric heat capacity of jellyroll, ($\text{J m}^{-3} \text{K}^{-1}$)	$\text{Rho} \cdot C_{p,batt}$	$2.789E6$
Average jelly roll radial thermal conductivity, W/cm K	$k_{T,batt}$	0.034
Heat transfer coefficient, $\text{W}/(\text{m}^2 \cdot \text{K})$	h_{conv}	7.17
Reaction heat, $\text{J} \cdot \text{kg}^{-1}$	H_{sei}	2.57×10^5
	H_a	1.714×10^6
	H_c	3.14×10^5

	H_e	1.55×10^5
Reaction frequency factor, s^{-1}	A_{sei}	1.667×10^{15}
	A_a	2.5×10^{13}
	A_c	6.667×10^{13}
	A_e	5.14×10^{25}
Reaction activation energy, $J \cdot mol^{-1}$	$E_{a_{sei}}$	1.3508×10^5
	E_{a_a}	1.3508×10^5
	E_{a_c}	1.396×10^5
	E_{a_e}	2.74×10^5
Initial value, dimensionless	$C_{0,sei}$	0.15
	$C_{0,a}$	0.75
	α_0	0.04
	$C_{0,e}$	1
Reaction order	m_{sei}	1
	$m_{a,n}$	1
	$m_{c,p1}$	1
	$m_{c,p2}$	1
	m_e	1
Volume-specific content of reacting material, $kg \cdot m^{-3}$	$t_{0,sei}$	0.033
	W_a	610
	W_c	1300
	W_e	406

Table 3. Initial concentrations and reaction rates for each component in Kim et al. (Kim et al., 2007) mechanism.

Component	Initial concentration	$-dc/dt$
Anode	0.75	$-R_{an}$
Cathode	0.04	$-R_{cat}$
Electrolyte	1	$-R_e$
SEI	0.15	$-R_{sei}$
t_{sei}	0.033	$-R_{an}$
Binder	-	-

3. RESULTS AND DISCUSSION

The TR simulation of the li-ion battery cells with different cathode, anode and electrolyte materials is performed to investigate the thermal stability and safety of li-ion batteries with different materials. The thermal stability of Li-ion batteries is characterized by the onset temperature and time of TR events. In addition, the thermal safety of the TR process can be characterized by the heat rate and peak temperature. The thermal safety of li-ion battery cell with LiCoO₂ cathode, graphite anode and standard LiPF₆ electrolyte is assessed based on Kim et al. kinetic mechanism. The results illustrated in Fig.4 indicate that battery cells are not prone to TR event at the temperatures under 150 °C. However, higher temperatures cause the start of exothermic reactions and further increased temperature. It can be found that higher temperatures can cause more serious hazard TR events in terms of released heat, temperature peak and onset time of TR. The results of temperature diagram, heat rate and average values for components are presented in Fig. 4.

The thermal safety of Li_{1.1}(Ni_{1/3}Co_{1/3}Mn_{1/3})_{0.9}O₂ battery cathode with standard LiPF₆ electrolyte and graphite anode is evaluated in Fig. 5. Unlike batteries with LiCoO₂ cathodes that presented temperature threshold of 150 °C, Li_{1.1}(Ni_{1/3}Co_{1/3}Mn_{1/3})_{0.9}O₂ batteries do not undergo TR process at temperatures below 170 °C. However, the thermal runaway events are much more intensive and oven temperatures of 180 can result in peak temperatures of 443 °C while LiCoO₂ batteries peak at ≈300 °C during TR at the same oven

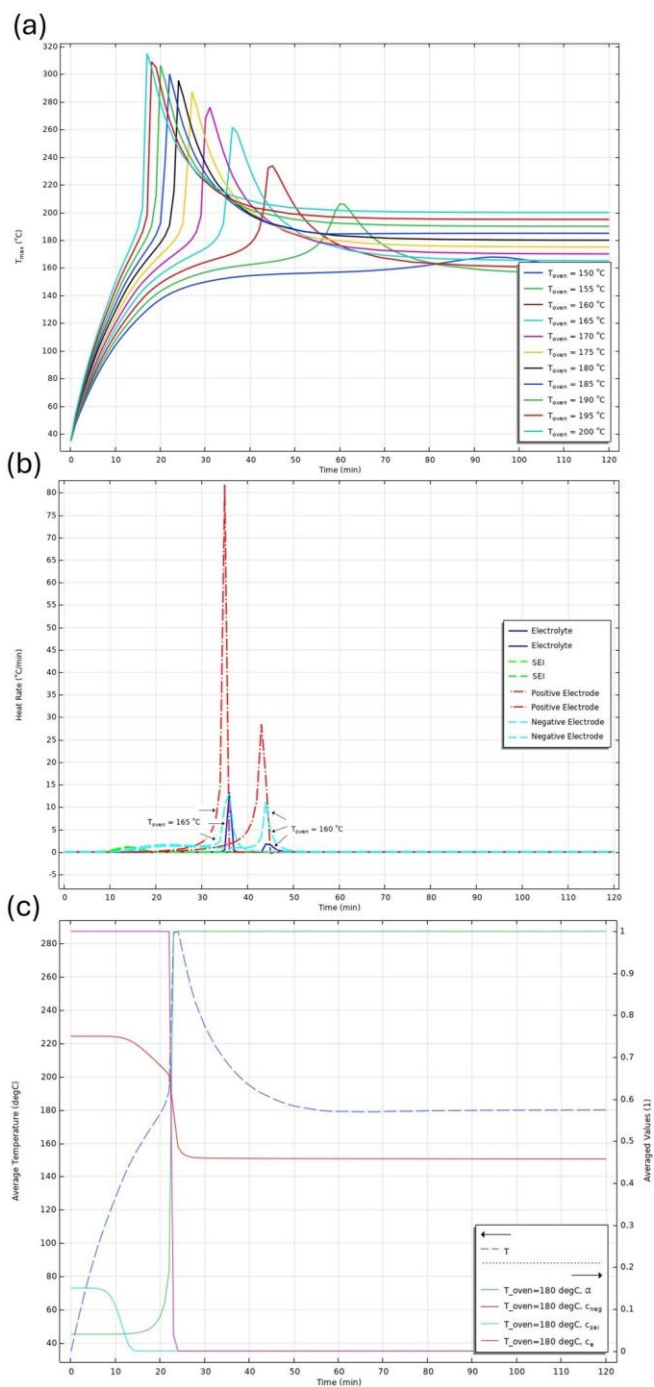


Fig. 4. TR kinetic mechanisms for LiCoO₂ battery with standard LiPF₆ electrolyte and graphite anode. A) Maximum temperature for Oven Temperature 150-200 °C B) Heating rate for Oven Temperature 160 and 165 °C C) Average values and temperature for Oven Temperature 180 °C.

The thermal safety of Li_{1.1}(Ni_{1/3}Co_{1/3}Mn_{1/3})_{0.9}O₂ battery cathode with standard LiPF₆ electrolyte and graphite anode is evaluated in Fig. 5. Unlike batteries with LiCoO₂ cathodes that presented temperature threshold of 150 °C, Li_{1.1}(Ni_{1/3}Co_{1/3}Mn_{1/3})_{0.9}O₂ batteries do not undergo TR process at temperatures below 170 °C. However, the thermal runaway events are much more intensive and oven temperatures of 180 can result in peak temperatures of 443 °C while LiCoO₂ batteries peak at ≈300 °C during TR at the same oven

temperature. The results of temperature diagram and heat rates for $\text{Li}_{1.1}(\text{Ni}_{1/3}\text{Co}_{1/3}\text{Mn}_{1/3})_{0.9}\text{O}_2$ batteries are presented in Fig. 5.

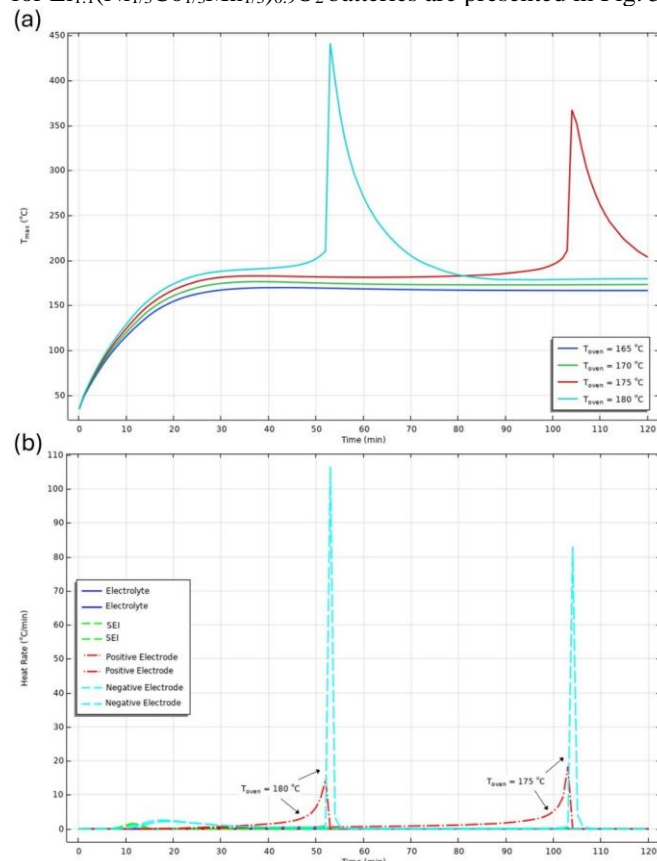


Fig. 5. TR kinetic mechanisms for $\text{Li}_{1.1}(\text{Ni}_{1/3}\text{Co}_{1/3}\text{Mn}_{1/3})_{0.9}\text{O}_2$ battery with standard LiPF_6 electrolyte and graphite anode A) Maximum temperature for Oven Temperature 165-180 °C B) Heating rate for Oven Temperature 175 and 180 °C.

The thermal safety of LiCoO_2 batteries with LiPF_6/PC : DMC electrolyte and standard graphite anode was also assessed in this study to compare the influence of different electrolyte materials. The results indicate that batteries undergo TR process at 150 °C while this is a safe temperature for $\text{Li}_{1.1}(\text{Ni}_{1/3}\text{Co}_{1/3}\text{Mn}_{1/3})_{0.9}\text{O}_2$ batteries or even LiCoO_2 batteries. The temperature peak is less substantial in LiCoO_2 batteries with LiPF_6/PC : DMC electrolyte compared to $\text{Li}_{1.1}(\text{Ni}_{1/3}\text{Co}_{1/3}\text{Mn}_{1/3})_{0.9}\text{O}_2$ batteries, but more intensive compared to LiCoO_2 batteries, especially at higher oven temperatures. The results of temperature diagram and heat rates for LiCoO_2 batteries with LiPF_6/PC : DMC electrolyte is presented in Fig. 6.

Lastly, thermal safety of LiCoO_2 batteries with standard LiPF_6 electrolyte and Lithiated $\text{Li}_4\text{Ti}_5\text{O}_{12}$ anode is assessed in this study to compare the influence of different anode materials. The results indicate that batteries undergo TR process at 160 °C. LiCoO_2 batteries with Lithiated $\text{Li}_4\text{Ti}_5\text{O}_{12}$ anode show less intensive TR process compared to all the previous battery types. This is evident from comparison of temperature peaks for different battery materials. The results of temperature diagram and heat rates for LiCoO_2 batteries with Lithiated $\text{Li}_4\text{Ti}_5\text{O}_{12}$ anode are presented in Fig. 7.

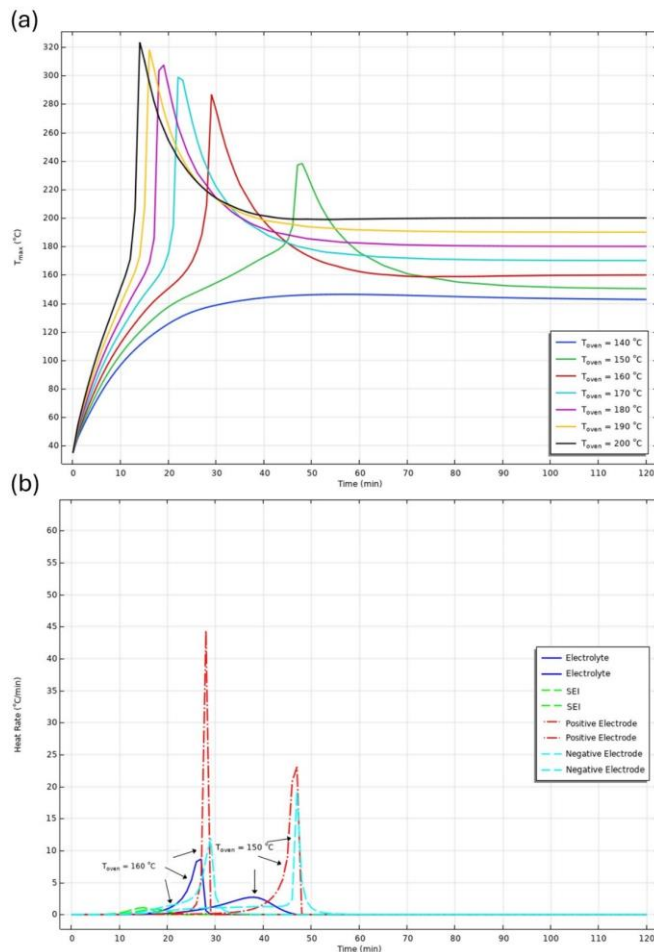


Fig. 6. TR kinetic mechanisms for LiCoO_2 battery with LiPF_6/PC : DMC electrolyte and graphite anode. A) Maximum temperature for Oven Temperature 140-200 °C B) Heating rate for Oven Temperature 150 and 160 °C.

4. CONCLUSIONS

In this study thermal stability of different battery materials was evaluated for li-ion batteries under thermal abuse conditions. A LiCoO_2 battery with standard LiPF_6 electrolyte and graphite anode is selected for oven test as the basic battery. Furthermore, a $\text{Li}_{1.1}(\text{Ni}_{1/3}\text{Co}_{1/3}\text{Mn}_{1/3})_{0.9}\text{O}_2$ cathode, LiPF_6/PC : DMC electrolyte and lithiated $\text{Li}_4\text{Ti}_5\text{O}_{12}$ anode is selected to assess the effect of different cathode, electrolyte and anode material on the thermal stability of the cell during thermal abuse conditions respectively. The results of temperature evolution and heat rate diagram are reported and comparison between different battery materials has been drawn.

It is shown that unlike batteries with LiCoO_2 cathodes with temperature threshold of 150 °C, $\text{Li}_{1.1}(\text{Ni}_{1/3}\text{Co}_{1/3}\text{Mn}_{1/3})_{0.9}\text{O}_2$ batteries do not undergo TR process at oven temperatures below 170 °C. However, the temperature peaks are more substantial in batteries with this type of cathode. Moreover, the temperature peak is more intensive in LiCoO_2 batteries with LiPF_6/PC : DMC electrolyte compared to the same battery with standard electrolyte but less intensive compared to $\text{Li}_{1.1}(\text{Ni}_{1/3}\text{Co}_{1/3}\text{Mn}_{1/3})_{0.9}\text{O}_2$ batteries. In addition, batteries with Lithiated $\text{Li}_4\text{Ti}_5\text{O}_{12}$ anode show less intensive TR process compared to all the previous battery types.

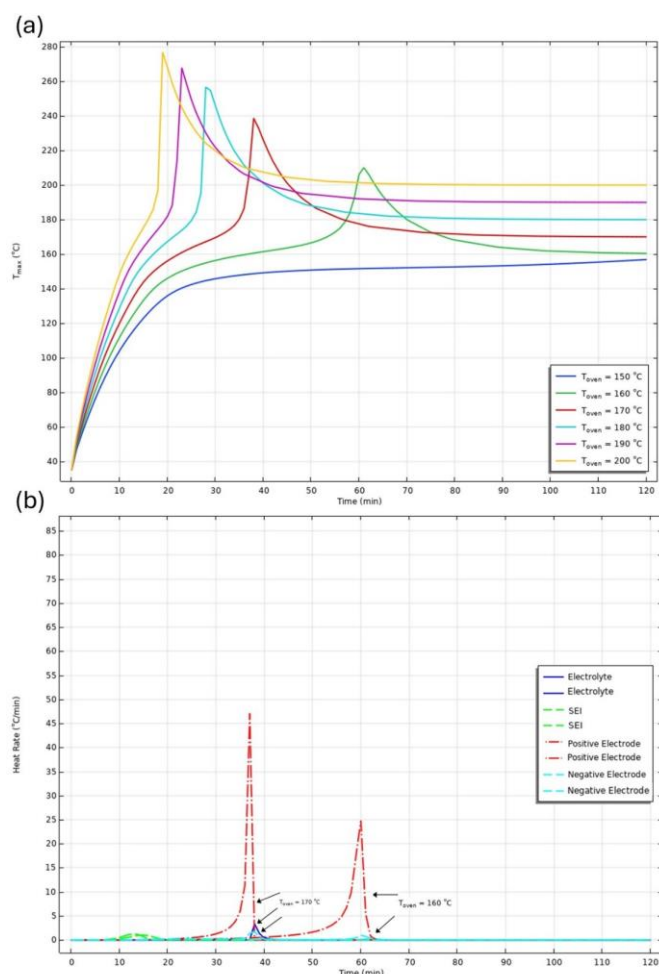


Fig. 7. TR kinetic mechanisms for LiCoO₂ battery with standard LiPF₆ electrolyte and Lithiated Li₄Ti₅O₁₂ anode A) Maximum temperature for Oven Temperature 140-200 °C B) Heating rate for Oven Temperature 160 and 170 °C.

The result of this study provides battery safety researchers with new insights into the thermal stability of different battery types. Further investigation into the assessment of battery materials thermal stability will foster the EV battery safety.

REFERNCIES

IEA (2024), Global EV Outlook 2024, IEA, Paris <https://www.iea.org/reports/global-ev-outlook-2024>, Licence: CC BY 4.0.

Wang, Y., Feng, X., Huang, W., He, X., Wang, L., and Ouyang, M. (2023). Challenges and opportunities to mitigate the catastrophic thermal runaway of high-energy batteries, *Advanced Energy Materials*, 13(15), 2203841. [doi:10.1002/aenm.202203841](https://doi.org/10.1002/aenm.202203841)

Gharehghani, A., Gholami, J., Shamsizadeh, P., and Mehranfar, S. (2022). Effect analysis on performance improvement of battery thermal management in cold weather, *Journal of Energy Storage*, 45, 103728. [doi:10.1016/j.est.2021.103728](https://doi.org/10.1016/j.est.2021.103728)

Rabiei, M., Gharehghani, A., and Andwari, A.M. (2023). Enhancement of battery thermal management system using a

novel structure of hybrid liquid cold plate, *Applied Thermal Engineering*, 232, 121051. [doi:10.1016/j.applthermaleng.2023.121051](https://doi.org/10.1016/j.applthermaleng.2023.121051)

Hatchard, T. D., MacNeil, D. D., Basu, A., and Dahn, J. R. (2001). Thermal model of cylindrical and prismatic lithium-ion cells, *Journal of The Electrochemical Society*, 148(7), A755. [doi:10.1149/1.1377592](https://doi.org/10.1149/1.1377592)

MacNeil, D. D., Lu, Z., Chen, Z., and Dahn, J. R. (2002). A comparison of the electrode/electrolyte reaction at elevated temperatures for various Li-ion battery cathodes, *Journal of power sources*, 108(1-2), 8-14. [doi:10.1016/S0378-7753\(01\)01013-8](https://doi.org/10.1016/S0378-7753(01)01013-8)

Peng, P., and Jiang, F. (2016). Thermal safety of lithium-ion batteries with various cathode materials: A numerical study, *International Journal of Heat and Mass Transfer*, 103, 1008-1016. [doi:10.1016/j.ijheatmasstransfer.2016.07.088](https://doi.org/10.1016/j.ijheatmasstransfer.2016.07.088)

Wang, Q., Sun, J., Yao, X., and Chen, C. (2006). Micro calorimeter study on the thermal stability of lithium-ion battery electrolytes, *Journal of Loss Prevention in the Process Industries*, 19(6), 561-569. [doi:10.1016/j.jlp.2006.02.002](https://doi.org/10.1016/j.jlp.2006.02.002)

Huang, P., Ping, P., Li, K., Chen, H., Wang, Q., Wen, J., and Sun, J. (2016). Experimental and modeling analysis of thermal runaway propagation over the large format energy storage battery module with Li₄Ti₅O₁₂ anode, *Applied energy*, 183, 659-673. [doi:10.1016/j.apenergy.2016.08.160](https://doi.org/10.1016/j.apenergy.2016.08.160)

Kong, D., Wang, G., Ping, P., and Wen, J. (2021). Numerical investigation of thermal runaway behavior of lithium-ion batteries with different battery materials and heating conditions, *Applied Thermal Engineering*, 189, 116661. [doi:10.1016/j.applthermaleng.2021.116661](https://doi.org/10.1016/j.applthermaleng.2021.116661)

Kim, G. H., Pesaran, A., and Spotnitz, R. (2007). A three-dimensional thermal abuse model for lithium-ion cells, *Journal of power sources*, 170(2), 476-489. [doi:10.1016/j.jpowsour.2007.04.018](https://doi.org/10.1016/j.jpowsour.2007.04.018)